

¹⁰A related linear stability calculation to explain the wavy instability of Bénard convection rolls has been given by R. M. Clever and F. H. Busse, *J. Fluid Mech.* **65**, 625 (1974).

¹¹The stability calculations exploit symmetries in y and z consistent with the Navier-Stokes equations. The fastest growing mode for the particular set of symmetries assumed here has $\text{Im}(\sigma) = 0$, and as a re-

sult G_x, G_z can be taken real and G_y pure imaginary. This reduces the computational work considerably. We use 33 Chebyshev polynomials in z for each of the two Fourier modes in x , resulting in a 106×106 (real) matrix eigenvalue problem. Further details will be published elsewhere.

¹²E. C. Bullard and H. Gellman, *Phil. Trans. Roy. Soc. London, Ser. A* **247**, 213 (1954).

Dynamics of Cavitons at Critical Density

E. W. Laedke and K. H. Spatschek

Fachbereich Physik, Universität Essen, D-4300 Essen, Federal Republic of Germany

(Received 10 March 1980)

The dynamics of envelope solitons accompanied by density depressions (cavitons) is analyzed with use of the driven Zakharov equations for inhomogeneous plasmas. The new contributions due to ion inertia as well as the novel phenomenon of amplitude-width-symmetry breaking are discussed. The results are applied to resonance absorption processes in laser-produced plasmas.

PACS numbers: 52.35.Mw

In an inhomogeneous plasma, conversion of electromagnetic waves into electrostatic waves enhances the field strengths of the latter by several orders of magnitude in the vicinity of the resonant layer, where the incident frequency matches the local plasma frequency. The amplitude swelling is due to the reduction of the group velocity from the velocity of light c to the electron thermal velocity v_{the} . The enhancement factor is approximately $(c/v_{\text{the}})^{1/2}$, and thus nonlinear effects¹ play an important role.

The importance of radiation-pressure effects in laser-plasma interaction has been demonstrated by particle simulations.² According to these results, a variety of processes occur at critical density. Some of the most important are resonant heating of electrons and generation of supra-thermal particles, strong steepening of density profile, etc. In the past, simplified analytical models^{2,3} have been proposed to explain these basic physical phenomena. In this Letter, we focus on one of them, i.e., profile steepening. A similar problem was studied in Ref. 3, where profile steepening because of cavity formation could be predicted. However, the calculations were based on the driven nonlinear Schrödinger equation ignoring ion inertia. We believe that ion inertia effects can become important. For example, in the static approximation ($\partial n/\partial t \approx 0$), it was found that a soliton would be strongly accelerated down the density gradient reaching even

electron thermal velocities. We expect that because of coupling with ions, the acceleration should be much smaller than predicted by the cubic nonlinear Schrödinger equation. Then the soliton stays for a longer time in the resonant region. Since position, velocity, phase detuning, etc., are coupled in a highly nontrivial manner, the problem of profile steepening at the critical density in laser-created plasmas via soliton formation has to be reconsidered.

The formulation presented here consists of describing the evolution of the electric field E through the nonlinear Schrödinger equation in which the density modification n is obtained from the ion-acoustic wave equation with the effects of the ponderomotive force included self-consistently. Thus, in the one-dimensional electrostatic approximation and for small driving fields E_d , the basic equations are

$$i\epsilon \partial E/\partial t + \partial^2 E/\partial x^2 - (\alpha x + n)E = E_d, \quad (1)$$

$$\partial n/\partial t = -\partial u/\partial x, \quad (2)$$

$$\partial u/\partial t = -(\partial/\partial x)(n + EE^*). \quad (3)$$

Here, the following units are used: time, $\sqrt{3}/\omega_{pi}$, where ω_{pi} is the ion plasma frequency; length, $\sqrt{3}\lambda_e$, where λ_e is the electron Debye radius; potential, T_e/e ; density, N_0 ; electric field, $(4\pi N_0 T_e)^{1/2}$; and velocity, $c_s = (T_e/m_i)^{1/2}$. Because of this normalization the parameter $\epsilon = 2(m_e/3m_i)^{1/2}$ appears in Eq. (1). In actual experiments

the initial spatial inhomogeneity length scale $L = \lambda_e/\alpha$ is of order $10^3\lambda_e$ and E_d is of order α . We want to emphasize that our analytical model is certainly too simple in order to lay claim to a complete consistent description of resonant absorption in laser plasmas. However, we believe that it models correctly the profile steepening process in nonisotropic (one-dimensional) laser plasmas. The applicability of one-dimensional models for the general problem of soliton propagation in perturbed systems has also been dis-

cussed.⁴

In order to solve Eqs. (1)–(3), we apply the approximative but powerful momentum method.^{3,5} The following modified conservation laws are used: For the plasmon number,

$$i\epsilon(\partial/\partial t)\int EE^*dx = -E_d\int(E - E^*)dx; \quad (4)$$

for the total momentum,

$$(\partial/\partial t)\int(i\epsilon E\partial E^*/\partial x + nu)dx = -\alpha\int EE^*dx; \quad (5)$$

and for the energy,

$$\int[(\partial E/\partial x)\partial E^*/\partial x + nEE^* + \frac{1}{2}n^2 + \frac{1}{2}u^2]dx = -\alpha\int xEE^*dx - E_d\int(E + E^*)dx + \text{const.} \quad (6)$$

In addition, the equations for the center of gravity of the motion,

$$i\epsilon(\partial/\partial t)\int xEE^*dx = -\int[2E\partial E^*/\partial x + xE_d(E - E^*)]dx, \quad (7)$$

and for the phase ψ of E ,

$$-\epsilon\int(\partial\psi/\partial t)EE^*dx = \int[(\partial E/\partial x)\partial E^*/\partial x + (\alpha x + n)EE^* + \frac{1}{2}E_d(E + E^*)]dx, \quad (8)$$

are taken into account.

For E , n , and u , we make the usual adiabatic approximation. Adiabaticity is a good assumption as long as the time needed by sound waves to traverse the soliton is small compared with the characteristic time for changes in the system. For physically relevant parameters, our results are consistent with that assumption. Introducing the five time-dependent parameters x_0 , q , η , a , and b , we use⁶ in the momentum equations

$$E = \sqrt{2}(1 - \dot{x}_0^2)^{1/2}q\eta\text{sech}[\eta(x - x_0)]\exp[i(ax + b)], \quad (9a)$$

$$n = -2\eta^2q^2\text{sech}^2[\eta(x - x_0)], \quad (9b)$$

$$u = -2\eta^2q^2\dot{x}_0\text{sech}^2[\eta(x - x_0)], \quad (9c)$$

where the dot denotes derivative with respect to time. Note that in this *Ansatz* velocity, amplitude, width, as well as the phase of the soliton are free. Inserting (9) into (4)–(8), one gets five coupled ordinary differential equations.

To quantify the influence of ions, we first treat the case $E_d = 0$. Then the differential equations could be solved analytically, and two different types of solutions were found: In the first case, $q = 1$ and $\eta \sim (1 - \dot{x}_0^2)^{-1}$ for all times whereas in the other one, $\eta = \eta_0$ is a constant and $q \sim (1 - \dot{x}_0^2)^{-1/2}$. Obviously, only the latter solution is stable; the first one is unstable with respect to small-amplitude perturbations.

For the stable solution, the relation between the velocity $v = \dot{x}_0$ and time t is

$$t = -\epsilon^2v/2\alpha - 4\eta_0^2v/3\alpha(1 - v^2)^2, \quad (10)$$

where we used $v(t=0) = 0$ as initial value. The velocity approaches the sound velocity very slowly from below (see dashed line in Fig. 1). Comparison of our result (10) with the corresponding one of Chukbar and Yankov,⁷ who analyzed non-

driven solitons by a completely different method, shows excellent agreement.

For applications to laser-fusion devices, the

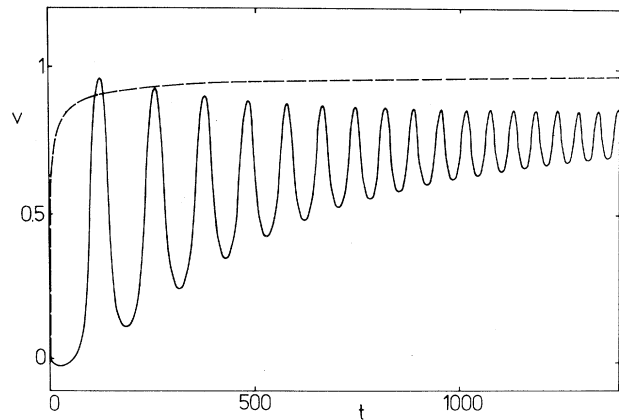


FIG. 1. Plot of the velocity v (in units c_s) vs time t (in units $2/\omega_{pe}$) for $\alpha = 0.003$ and $E_d = 0.0043$. The broken line depicts the result for $E_d = 0$.

computations for $E_d \neq 0$ are new and of utmost interest. Our solutions of the five ordinary differential equations show the following general behavior. The soliton formed will have its height increasing because of the energy input due to the driver. The soliton saturates when it moves out of the resonance region due to acceleration in the density gradient. So far the behavior is expected. However, new effects changing the physical conclusions for, e.g., saturation values and profile modification appear. We will first discuss the phenomena of ion drag and amplitude-width-symmetry breaking.

The acceleration and thereby the velocity of a soliton are strongly influenced by ion mass effects. In Fig. 1 we have displayed the time variation of the velocity. After an initial phase, the averaged velocity approaches the result given by (10) for $E_d = 0$. The velocity is always smaller than c_s whereas previously⁸ it became larger than v_{ie} . Correspondingly, previously the soliton has traveled over many Debye lengths and thereby presumably left the resonance region before saturation could occur. In the present case, the

position of the soliton is shifted only by a few Debye lengths. This occurs since actually the electrons are tied to the ions via the ambipolar field; the effective ion drag hinders the soliton from reaching sound velocity.

The width of the soliton η^{-1} turns out to be constant in time. This effect was detected by use of a generalized Ansatz for the soliton shape. The result is that the driver breaks the amplitude-width symmetry assumed previously, i.e., the width is not anymore inversely proportional to the amplitude. This at the first moment surprising outcome of our general nonlinear investigation is also true in the linear regime as will be shown now. To be consistent with the adiabatic approximation of the nonlinear calculation we have to choose an adiabatically turned on driver [$E_d - E_d \exp(\gamma t)$ for $-\infty < t \leq 0$ with $\gamma \geq 0$; γ^{-1} can be interpreted as the finite rise time of the laser pulse]. After transforming the spatial inhomogeneity in the usual manner, the linear equation

$$i\epsilon \frac{\partial E}{\partial t} + \frac{\partial^2 E}{\partial x^2} = E_d \exp\left(\frac{i\alpha t x}{\epsilon} - \frac{2i\alpha^2 t^3}{3\epsilon^3} + \gamma t\right), \quad (11)$$

can be solved by Green's-function method,

$$G(x, t; x', t') = -i [4\pi i \epsilon (t - t')]^{-1/2} \exp\left[i \frac{\epsilon(x - x')^2}{2(t - t')}\right]. \quad (12)$$

We find a solution of constant width

$$E(x, t) = iE_d e^{\gamma t} \int_0^\infty \exp\left(-\frac{1}{3}i\alpha^2 \tau^3 - i\alpha x \tau - \epsilon \gamma \tau\right) d\tau. \quad (13)$$

The inverse width of (13) is of order

$$\eta \simeq \pi\alpha / 4\epsilon\gamma. \quad (14)$$

We can use expression (14) as an initial value for our nonlinear solution. Since in the latter the width remains unchanged, Eq. (14) also predicts the scaling of the final soliton width, in terms of the inhomogeneity scale length and pump shape.

Let us now discuss the implications for energy saturation and profile steepening. In Fig. 2, the relaxation and saturation behavior of the field energy is shown. We first observe that the field energy reaches a peak on the ion time scale. Saturation occurs after many ion periods and not as predicted previously on the electron time scale. This is now expected since because of the ion drag the total density has to adjust itself to the radiation pressure. As a consequence of ion inertia and constant soliton width saturation occurs at a lower level (about 50%) than calculated previously. Furthermore, pronounced relaxation oscillations appear. They can be understood from the asymptotic form (large t) of the energy equation

$$\frac{dW}{dt} \simeq -\frac{\pi}{\sqrt{2}\epsilon} E_d \left(\frac{W}{\eta}\right)^{1/2} \sin\left(-\frac{\pi}{2} + \frac{\alpha}{2} \frac{t^2}{\epsilon}\right) \quad (15)$$

with $W \equiv \frac{1}{4} \int E E^* dx = q^2 \eta (1 - \dot{x}_0^2)$.

The solution of (15) is

$$W^{1/2} \simeq [W(t_0)]^{1/2} + \frac{\pi^{3/2} E_d}{2^{3/2} \alpha^{1/2} \epsilon^{1/2} \eta^{1/2}} \left[C\left(\frac{\alpha^{1/2} t}{\pi^{1/2} \epsilon^{1/2}}\right) - C\left(\frac{\alpha^{1/2} t_0}{\pi^{1/2} \epsilon^{1/2}}\right) \right], \quad (16)$$

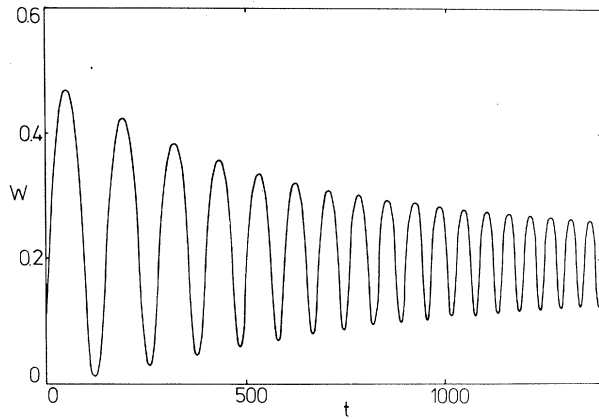


FIG. 2. $W \left(\frac{1}{2} \int |E|^2 dx \right)$ in units $4\sqrt{3}\pi N_0 T_e \lambda_e$ vs t (in units $2/\omega_{pe}$) for the same parameters as in Fig. 1.

where $C(z)$ is the Fresnel integral. From (16) we see that the characteristic frequency at the n th maximum,

$$\omega_n = 2\pi/(\Delta t)_n \simeq (8\pi n \alpha / \epsilon)^{1/2} \quad (17)$$

scales as $\alpha^{1/2}$.

The density depression $\delta n \equiv n_\infty - n_{\min} = 2\eta^2 q^2$ does not show large relaxation oscillations. As is seen from Fig. 3, it slowly increases with time. Again, the ion drag is responsible for the different behavior of the relaxation oscillations compared to the electric field. Because of the coupling with the heavy ions, the response of the fluid density to radiation pressure oscillations is quite moderate. Taking the ratio of averaged field intensity and corresponding density depression we find that less radiation will be trapped in the caviton, compared to the static approximation result. Furthermore, the size of the caviton determines the profile modification at resonance. Estimating the local density gradient due to caviton formation by $2q^2\eta^3$ we recognize that steepening factors of order 5 are reasonable for physically relevant parameters. In the long run, transverse instabilities can cause density rippling. Because of the dynamic ions, spatial anisotropy, and the probably generated strong magnetic fields, these instabilities⁹ as well as the collapse as their final state are less important than in iso-

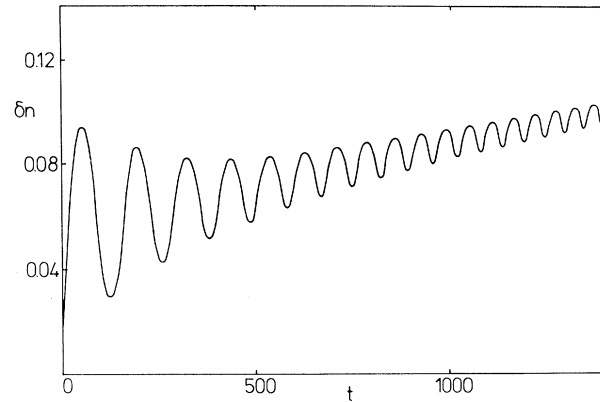


FIG. 3. Absolute maximum density depression δn (in units N_0) vs t (in units $2/\omega_{pe}$) for the same parameters as in Fig. 1.

tropic Schrödinger systems.¹⁰

This research was supported by the Deutsche Forschungsgemeinschaft under Sondersforschungsbereich 162.

¹V. I. Karpman and E. M. Krushkal, Zh. Eksp. Teor. Fiz. **55**, 530 (1968) [Sov. Phys. JETP **28**, 277 (1969)].

²D. W. Forslund, J. M. Kindel, and K. Lee, Phys. Rev. Lett. **39**, 284 (1977); K. Estabrook and W. L. Kruer, Phys. Rev. Lett. **40**, 42 (1978); B. Bezzerides, S. J. Gitomer, and D. W. Forslund, Phys. Rev. Lett. **44**, 651 (1980).

³H. H. Chen and C. S. Liu, Phys. Rev. Lett. **39**, 1147 (1977).

⁴A. Bondeson, Phys. Fluids **23**, 746 (1980).

⁵D. R. Nicholson and M. V. Goldman, Phys. Fluids **19**, 1621 (1976).

⁶According to Chen and Liu, Ref. 3, the threshold driving field for N -soliton formation is $N + \frac{1}{2} > E_d / \sqrt{2}\alpha > N - \frac{1}{2}$, so that for $E_d \simeq \alpha$ a one-soliton Ansatz is justified.

⁷K. V. Chukbar and V. V. Yankov, Fiz. Plazmy **3**, 1398 (1977) [Sov. J. Plasma Phys. **3**, 780 (1977)].

⁸Calculations for the parameters used in Ref. 3 give plots qualitatively similar to Figs. 1-3.

⁹E. W. Laedke and K. H. Spatschek, Phys. Rev. Lett. **41**, 1798 (1978), and **42**, 1534 (1979).

¹⁰V. E. Zakharov, Zh. Eksp. Teor. Fiz. **62**, 1745 (1972) [Sov. Phys. JETP **35**, 908 (1972)].